SEISMIC RELIABILITY ASSESSMENT OF EXISTING R/C FLAT-SLAB BUILDINGS

By Y. H. Luo,[1] Associate Member, ASCE, A. Durrani,[2] and J. Conte,[3] Members, ASCE

ABSTRACT: The reliability of existing reinforced-concrete flat-slab buildings, designed and detailed to resist gravity loads only, was studied for punching failure at connections under earthquake-type loading. Two flat-slab buildings, three and 10 stories in height, designed according to the ACI 318-56 building code, were used in the nonlinear dynamic analysis and reliability calculations. Results from previous experimental results on the seismic resistance of slab-column connections were employed to establish the effective slab widths, unbalanced moment-transfer capacity of connections, and their punching strength. The member dimensions, material strengths, and live load were treated as random variables and the effect of model uncertainty was included in the calculations of reliability indices. Random earthquake time histories were generated with the Kanai-Tajimi power spectrum. The limit-state function was based on the punching failure capacity of the interior slab-column connections. Based on the reliability analysis, the probability of failure of existing flat-slab buildings are presented for different soil conditions and peak ground accelerations varying from $0.05g$ to $0.2g$.

INTRODUCTION

Flat-slab buildings in the eastern region of the United States have been typically designed for gravity and wind loads only and thus, may not have the ability to resist earthquakes of moderate intensity without severe damage. The buildings constructed prior to the 1960s (ACI 318-63) are regarded as being particularly vulnerable to earthquake loading. The slab-column connections in these buildings were not designed and detailed to withstand moment reversals, and do not have protection against progressive collapse in the event of a punching failure, i.e., the slab bottom reinforcement is not continuous through the column. The unbalanced moments at connections due to unsymmetrical gravity loads or lateral loads from wind or earthquakes were not considered in the design of older flat-slab buildings. As recognized by the present building code [ACI 318-89; *Building* (1989)], both unbalanced moment and gravity shear produce shear stresses at the connections, and the available gravity shear capacity decreases as the unbalanced moment increases. Experimental investigations (Durrani and Du 1992; Luo and Durrani 1994) have shown that the interior connections can fail in punching when subjected to high gravity shear and moment reversals. For connections without slab bottom reinforcement continuous through the column, as is the case in the older flat-slab buildings, the punching failure is not contained locally, which can result in progressive collapse of the building.

Concerns over the possibility of a moderate-intensity earthquake in the eastern region of the United States call for the evaluation of the potential damage to the older flat-slab buildings. Experience from the Mexico City earthquake ("Impressions" 1985) and the San Fernado earthquake ("CSMIP" 1987) have demonstrated the vulnerability to collapse of inadequately detailed flat-slab buildings when subjected to ground motions of moderate to strong intensity. The risk of punching failure at the connections and the potential for overall structural collapse need to be assessed before the development of effective retrofit strategies to improve the seismic safety of older flat-slab buildings.

This paper presents an analytical approach to assess the vulnerability of reinforced-concrete flat-slab buildings subjected to earthquakes. The inherent variability of material strengths and dimensions of concrete members, the model uncertainty, and the stochastic nature of live load are the main sources controlling the response uncertainty of a reinforced-concrete structure. The randomness and uncertainty of earthquakes significantly affect the likelihood of the damage sustained by the buildings. In this study, three-dimensional flat-slab buildings were modeled as lumped parallel plain frames, and the response of the frames subjected to ground motion was calculated by employing a nonlinear time-history analysis program, IDARC, developed for reinforced-concrete frame-wall structures (Kunnath et al. 1992). The material strengths and dimensions of concrete members, the model uncertainty, and the live load were modeled as random variables. Earthquake acceleration time histories were simulated from the Kanai-Tajimi power spectrum. The soil predominant frequency and viscous damping parameters in the Kanai-Tajimi power spectrum were selected based on previous investigations (Lai 1982; Sues et al. 1985). Synthetic earthquake ground motions were generated from the power spectrum using the spectral decomposition method and random phase angles uniformly distributed between 0 and 2π. The probability of punching failure at the interior connections for the synthetic ground motions was then calculated by nonlinear earthquake response analysis using IDARC and a general-purpose reliability-analysis program CALREL (Liu et al. 1989).

ANALYSIS MODEL FOR FLAT-SLAB STRUCTURES

Since probabilistic nonlinear finite-element analysis of reinforced-concrete buildings is computationally intensive, the analysis was carried out only for typical three- and 10-story flat-slab buildings as shown in Fig. 1. These buildings were designed according to the ACI 318-56 (*Building* 1956) for gravity loads only. The design dead load consisted of the slab self-weight, partition load of 20 psf (0.956 kPa), and mechanical attachments of 10 psf (0.478 kPa). The design live load was taken as 50 psf (2.39 kPa), which is typical for an office building. The slab bottom reinforcement at connections was detailed as in most of the older flat-slab buildings, i.e., the slab bottom reinforcement was not continuous through the interior columns and it extended only 6 in. into the exterior columns. As observed from tests on slab-column con-

[1]Struct. Engr., Zentech Inc., 8582 Katy Freeway, Houston, TX 77204.
[2]Prof., Dept. of Civ. Engrg., Rice Univ., P.O. Box 1892, Houston, TX 77251.
[3]Asst. Prof., Dept. of Civ. Engrg., Rice Univ., P.O. Box 1892, Houston, TX

Note. Associate Editor: Steven L. McCabe. Discussion open until March 1, 1996. To extend the closing date one month, a written request must be filed with the ASCE Manager of Journals. The manuscript for this paper was submitted for review and possible publication on February 22, 1994. This paper is part of the ***Journal of Structural Engineering***, Vol. 121, No. 10, October, 1995. ©ASCE, ISSN 0733-9445/95/0010-1522–1530/$2.00 + $.25 per page. Paper No. 7883.

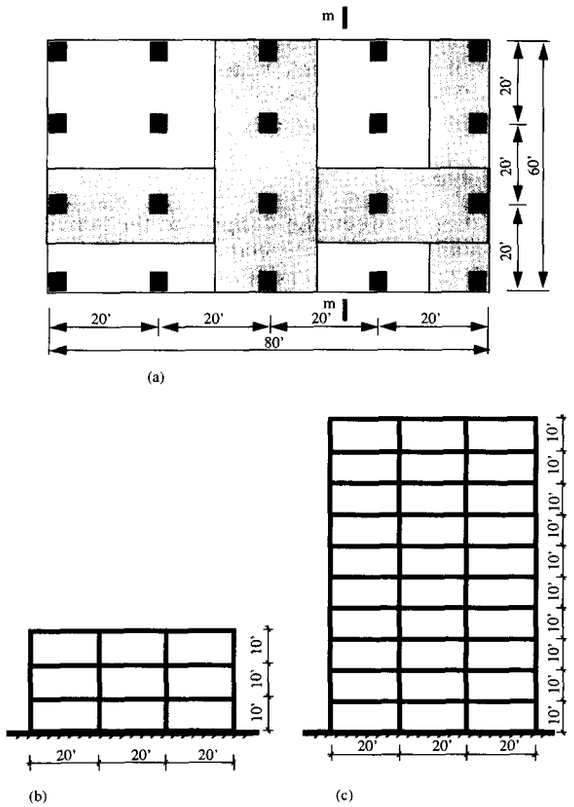

FIG. 1. Configuration of Flat-Slab Buildings (1 ft = 304.8 mm): (a) Floor Plan; (b) Elevation of Three-Story Building; (c) Elevation of 10-Story Building

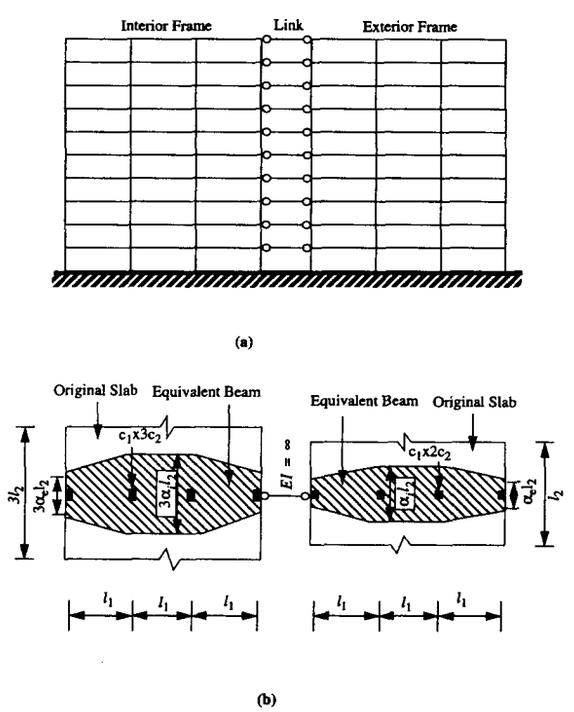

FIG. 2. Analysis Model of Flat-Slab Buildings: (a) Elevation; (b) Plan

nections subassemblies (Durrani and Du 1992; Luo and Durrani 1994), the moment-transfer capacity of the slab in positive bending was limited to the flexural cracking capacity at both the interior and exterior connections.

The flat-slab buildings under consideration are analyzed for seismic loading using the equivalent frame approach proposed by Luo et al. (1994). In this approach, a flat-slab building is modeled as a set of parallel plane frames in which the columns are modeled conventionally and the slabs are modeled as equivalent beams. The equivalent beam has a depth equal to that of the original slab and an effective width that targets both the strength and the stiffness of the slab. As shown in Fig. 1, the flat-slab building is idealized as independent sets of planar frames in the two orthogonal directions. Only frames in the weak direction, namely the transverse direction, were analyzed in this study. The building is modeled as a set of lumped interior and exterior frames coupled by means of hinged rigid links at all floor levels. Lumping of the frames, shown in Fig. 2, is achieved by adding the column areas and moments of inertia at the same column line and the beam moments of inertia at the same floor level. The interior frame thus has an effective beam width of $3\alpha_i l_2$ at interior connections and $3\alpha_e l_2$ at exterior connections, where α_i and α_e are the slab effective width factors at the interior and exterior connections, respectively, and l_2 is the panel width normal to the loading direction. Similarly, the exterior frame has an effective beam width of $\alpha_i l_2$ and $\alpha_e l_2$ at the interior and exterior connections, respectively. The lumped columns for the interior frames have a width of $3c_2$ and a depth of c_1, and the lumped columns for the exterior frame have a width and depth of $2c_2$ and c_1, respectively, where c_2 and c_1 are the width and depth of the original column. The effective slab-beam width factors, α_i and α_e, are obtained from (Luo and Durrani 1995)

$$\alpha_i = \chi \left\{ \frac{1.02[(c_1/l_2)]}{0.05 + 0.002[(l_1/l_2)]^4 - 2[(c_1/l_1)]^3 - 2.8[(c_1/l_1)]^2 + 1.1[(c_1/l_1)]} \right\} \quad (1)$$

$$\alpha_e = \chi \frac{K_t}{K_t + K_s} \quad (2)$$

where $\chi = [1 - 0.4(V_0/4A_c\sqrt{f'_c})]$ is a reduction factor accounting for the effect of gravity load; K_t = torsional stiffness of the slab edge and spandrel beams, if present, as defined in ACI 318-89 (*Building* 1989); and $K_s = (4E_{cs}I)/l_1$ is the flexural stiffness of the slab framing into the exterior connection.

ENSEMBLE OF EARTHQUAKE TIME HISTORIES

The Kanai-Tajimi filter is used to generate the frequency content of the ensemble of artifical earthquakes employed in this study. The Kanai-Tajimi power spectral density is defined as

$$S_g(\omega) = S_0 \frac{1 + 4\xi_g^2[(\omega/\omega_g)]^2}{\{1 - [(\omega/\omega_g)]^2\}^2 + 4\xi_g^2[\omega/\omega_g)]^2} \quad (3)$$

in which S_0 = amplitude of the spectrum related to the expected peak ground acceleration; ω_g = dominant ground frequency of the site soil; and ξ_g = critical damping of the site soil.

To generate an ensemble of synthetic accelerograms by the Kanai-Tajimi power spectrum, two parameters ω_g and ξ_g are needed. The values of these parameters, as proposed in earlier studies (Lai 1982; Sues et al. 1985; Hwang and Jaw 1990), vary significantly. By analyzing the accelerograms from 140 real strong ground motions, including 22 rock-site records and 118 soil-site records, Lai (1982) recommended a mean value for ω_g and ξ_g of 26.7 rad/s and 0.35, respectively, for rock sites, and 19.1 rad/s and 0.32 for soil sites. The coefficient of variation of ω_g and ξ_g was found to be 0.398 and 0.391,

respectively, for rock sites and 0.425 and 0.426 for soil sites. Sues et al. (1985) suggested ω_g and ξ_g parameter values of 10.9 rad/s and 0.96 for soft soil, 16.5 rad/s and 0.80 for intermediate soil, and 16.9 rad/s and 0.94 for hard soil. To examine the effects of these parameters on the failure probability, both set of parameters were used in this study.

Shinozuka (1974) showed that a stationary acceleration time history can be generated from

$$a_s(t) = \sum_{n=1}^{N_f} [\sqrt{2S_g(\omega_n)\Delta\omega}\, \sin(\omega_n t + \Phi_n)] \quad (4)$$

in which the phase angles Φ_n, $n = 1, 2, \ldots, N_f$, represent N_f independent realizations of an underlying random variable uniformly distributed between 0 and 2π. The time-varying intensity typical of actual earthquake accelerograms is modeled by applying an envelope function to the stationary ground acceleration time history. The envelope function defined by Sues et al. (1985)

$$\psi(t) = [(t/t_1)]^2, (0 \le t \le t_1); \quad \psi(t) = 1, (t_1 \le t \le t_2) \quad (5a,b)$$

$$\psi(t) = e^{-0.18(t-t_2)}, (t_2 \le t) \quad (5c)$$

is adopted here where t_1 = rise time; and $t_2 - t_1$ = duration of the strong stationary phase. Based on the investigation of Moayyad and Mohraz (1982), Sues et al. (1985) recommended representative strong motion durations of 10.0 s, 7.0 s, and 5.5 s for soft-, intermediate- and hard-site soils, respectively. From their analysis of 140 actual earthquake records, Vanmarcke and Lai (1980) found a mean strong-motion duration of 5.1 s and 10.1 s for rock and soil sites, respectively. For each set of Kanai-Tajimi parameters, the aforementioned corresponding strong motion durations were used in the analysis.

RELIABILITY ANALYSIS

The failure probability P_f is the probability that the realization of the basic variables yields a point in the failure domain, i.e.

$$P_f = P[G(\mathbf{X}) \le 0] \quad (6)$$

where $\mathbf{X}$ = vector of basic variables; and $G(\mathbf{X})$ = limit-state function defined such that the region $\{G[(\mathbf{X}) \le 0]\}$ corresponds with the failure mode of interest. The corresponding reliability index β can be calculated from

$$\beta = -\phi^{-1}(P_f) \quad (7)$$

where ϕ^{-1} = inverse of the standard normal cumulative distribution function. The probability calculations were carried out with the general-purpose reliability-analysis program CALREL (Liu et al. 1989), which formulates the probabilistic model in the space of independent standard normal variables. This computer program provides estimates of the failure probability based on the analytical first- and second-order reliability methods (FORM and SORM, respectively), or based on simulation methods such as the basic Monte Carlo-simulation method or the more elaborate directional-simulation method. In this study, FORM and SORM were used to calculate the failure probability of flat-slab buildings under static loading. For the reliability analysis of flat-slab buildings under seismic loading, the FORM and SORM calculations did not converge due to the more complicated nature of the limit-state function (which becomes a functional) and of the failure region in the dynamic case. FORM/SORM reliability methods as applied to dynamic systems are still a subject of active research. Therefore, the Monte Carlo-simulation (MCS) method was used to calculate the failure probability in this case. The choice of MCS for the dynamic case is justified because the structural models used are quite simple and the failure probabilities computed are relatively high, which keeps the number of simulated time histories required to a reasonable level. When these conditions are not met, analytical random vibration methods are typically used.

Basic Variables

The variation between the design and the actual member dimensions and between the specified and the actual material strengths are the main sources of uncertainty of the capacity. The random nature of the seismic and live loads produces variability in the response of buildings. The variations in dimensions and material strengths, and the live load uncertainty are discussed in detail in the following sections.

Slab Thickness

A number of studies (Ellingwood and Ang 1974; Mirza and MacGregor 1979a) have shown that a normal distribution can be used to represent the variability of the geometric imperfections of reinforced-concrete members. As such, a normal distribution was assumed for the slab thickness in this study. Based on the statistical analysis of a large number of in-situ sample slabs, Mirza and MacGregor (1979a) concluded that the mean deviation from the nominal values of the slab thickness was negligible. By analyzing a subset of their data applicable to flat slabs, the nominal value for the slab thickness was taken as the mean value of the distribution with a coefficient of variation of 0.067.

Effective Depth of Slab

In flat-slab buildings, the effective depth of slab directly affects the punching capacity at slab-column connections. The effective depth variability is, therefore, an important source of uncertainty in estimating the punching capacity. Several studies (Fiorato 1973; Mirza and MacGregor 1979a) showed that the average depth of the top and bottom bars measured relative to the slab bottom were smaller than the nominal dimensions. The depth of the top reinforcement was more affected than the bottom bars because construction personnel were walking on the top reinforcement during steel placement and concreting operations. For the depth of the slab top reinforcement, Mirza and MacGregor (1979a) recommended a normal distribution with a mean deviating from the nominal value by -0.77 in. (-1.96 cm) and a standard deviation of 0.63 inch (1.6 cm). By analyzing their data applicable to flat slabs, a mean deviation of $-0.13d_s$ and a standard deviation of $0.10d_s$, where d_s is the effective depth of the slab, were selected for the effective depth of the slab top reinforcement measured from the bottom face.

Column Dimensions

Mirza and MacGregor (1979a) showed that the variation of column size was relatively small compared with that of the slab thickness. They suggested a normal distribution with a mean equal to the nominal value and a standard deviation of 0.262 in. (0.66 cm), to represent the actual variability of column dimensions. These recommendations were also adopted for the reliability analysis of flat-slab buildings in this study.

Concrete Strength

A number of researchers, including Julian (1955), Mirza et al. (1979), and Ang and Cornell (1974), recommended the normal distribution to represent the variability of the compressive strength of concrete. Mirza et al. (1979) observed the actual strength of core concrete in structures to be gen-

erally lower than the standard cylinder strength due to the difference in placing, curing, and dimensions. The average ratio of core strength to standard cylinder strength was found to be around 0.85. The reduction in the in-situ strength of concrete, however, is partially offset because the existing design codes require the average cylinder strength to be about 700 to 900 psi (4.83 to 5.21 MPa) greater than the specified strength. They also suggested that the mean and standard deviation of the compressive strength of concrete can be predicted by

$$f = 0.675f'_c + 1{,}100 \leq 1.15f'_c \text{ (psi)} \tag{8}$$

$$V^2 = V^2_{c,\text{real}} + V^2_{\text{in-situ}} + V^2_R \tag{9}$$

where f'_c = design compressive strength of concrete; $V_{c,\text{real}}$ = variability (coefficient of variation) of the concrete strength in the structure with respect to cylinder strength; $V_{\text{in-situ}}$ = variability of the concrete strength in the structure with respect to the in-situ strength; and V_R = variability of the concrete strength in the structure due to a variable loading rate. For 3,000 psi (20.69 MPa) concrete, the mean and standard deviation obtained from (8) and (9) are 3,125 psi (21.55 MPA) and 469 psi (3.23 MPa), respectively. The punching shear capacity of slab-column connections depends on the splitting strength of concrete, which is treated as an independent random variable. A normal distribution with a mean of $6.4\sqrt{f'_c}$ (psi units) and a coefficient of variation of 0.18 was used to model the concrete splitting strength (Mirza et al. 1979; Lu et al. 1994).

Reinforcing Steel

Variations in the strength of steel and the cross-section area of the reinforcing bars are the main sources of variability for the yield strength of the steel bars. By analyzing data on steel yield strength from mill tests, Mirza and MacGregor (1979b) found that a beta distribution best represents the dispersion of the yield strength for Grade 40 steel. The mean and standard deviation of the yield strength for Grade 40 reinforcing bars were found to be 48.8 ksi (336.5 MPa) and 5.22 ksi (36 MPa), with the lower and upper bounds of the distribution being 36 ksi (248.2 MPa) and 68 ksi (468.9 MPa), respectively. Further, the actual area of reinforcing bars tends to deviate from the nominal area. Mirza and MacGregor (1979b) suggested that the dispersion of the ratio of measured to nominal areas can be approximately represented by a truncated normal distribution with a lower bound at 0.94, a mean value of 0.99, and a coefficient of variation of 2.4%.

Live Load

Based on the results of the first extensive load survey of office buildings in the United States organized by the National Bureau of Standards, Ellingwood and Culver (1977) found that the maximum live load in office buildings corresponding to a return period of 50 years, $L_{50\text{yr}}$, can be described by a type I extreme value distribution with mean and variance as follows

$$E(L_{50\text{yr}}) = 18.7 + 520/\sqrt{A} \text{ (psf)} \tag{10}$$

$$\text{var}(L_{50\text{yr}}) = 14.2 + 18.900/A \text{ (psf)}^2 \tag{11}$$

in which A = influence area. These values were used for the present reliability analysis of the representative flat-slab buildings under static loading.

Since the probability of simultaneous occurrence of the maximum live load and seismic load is relatively small, sustained live load is used for the seismic reliability analysis of flat-slab buildings. A number of researchers (Corotis and Doshi 1977; Ellingwood and Culver 1977) recommended that a gamma distribution be used to model the dispersion of live load for office buildings. Culver (1976) found that the magnitude of live load in office buildings was not affected by the geographic location of the building, the building height, and the age of the building. By analyzing the survey results of office buildings with areas of up to 3,800,000 ft^2 (353,400 m^2), Chalk and Corotis (1980) found that the mean and standard deviation of live load for office buildings were 10.9 psf (0.52 kPa) and 5.9 psf (0.28 kPa), respectively. From the survey results of 22,554 office rooms, Corotis and Doshi (1977) found a mean live load of 12.72 psf (0.61 kPa). These researchers found that the room area had a significant effect on the magnitude of live load per unit area. The average load per unit area generally decreased as the room area increased. Based on the procedure suggested by Ellingwood and Culver (1977), the mean and standard deviation of sustained live load for office occupancy, corresponding to an influence area of 400 ft^2 (37.2 m^2), were calculated to be 11.6 psf (0.56 kPa) and 7.87 psf (0.38 kPa), and were used in this study.

The basic random variables, their respective marginal distributions, and their distribution parameters are summarized in Table 1.

Limit-State Function

The limit-state function, $G(\mathbf{X})$ is the deterministic mechanical model describing the failure event of interest and is formulated as $G_i(\mathbf{X}) = R_i(\mathbf{X}) - L_i(\mathbf{X})$ in which $R_i(\mathbf{X})$ and $L_i(\mathbf{X})$ are the resistance and load effects, respectively, corresponding to the ith failure mode, which is the punching failure at the ith interior connection. The failure condition $G_i(\mathbf{X}) \leq 0$ defines the failure domain in the $\mathbf{X}$-parameter space. The load effect L_i was calculated for both gravity load only and for a combination of gravity and seismic loads. The uniform floor load was taken as $q = L + 12.5h_s + 10$ (psf), in which 10 psf (0.48 kPa) is assumed to be the average actual weight of partition plus mechanical attachments. Only the punching failure at the interior slab-column connections were considered in this study.

In older flat-slab buildings, which were designed to resist gravity loads only, punching failure at interior connections is likely to initiate the progressive collapse of the building. By testing slab-column connection subassemblies under quasi-

TABLE 1. Description of Random Variables

X_i (1)	Description (2)	Distribution (3)	Mean (4)	Standard deviation (5)
h_s	Slab thickness	Normal	h_s[a]	$0.067h_s$
d_{ave}	Effective slab depth	Normal	$0.87d_{\text{ave}}$	$0.10d_{\text{ave}}$
f_c	Compressive strength of concrete	Normal	3,125 (psi)	469 (psi)
f_{sp}	Splitting strength of concrete	Normal	$6.4\sqrt{f'_c}$	$1.15\sqrt{f'_c}$
A_s	Steel area	Normal	A_s	$0.024A_s$
f_y	Yield strength of steel	Beta	48.8 (ksi)	5.22 (ksi)
c_1	Column dimension	Normal	c_1	0.262 (in.)
c_2	Column dimension	Normal	c_2	0.262 (in.)
L_{sus}	Sustained live load	Gamma	11.6 (psf)	7.87 (psf)
$L_{50\text{yr}}$	Maximum live load within 50 years	Type I	44.7 (psf)	7.84 (psf)
$\tilde{B}$	Model uncertainty factor	Normal	1.00[b]/1.65[c]	0.12[b]/0.27[c]

[a]Nominal values; 1 in. = 25.4 mm; 1 psf = 47.9 kPa.
[b]Model uncertainty factor for punching at interior connections under combined lateral and gravity loads.
[c]Model uncertainty factor for punching at interior connections under gravity load only.

static loading, Durrani and Du (1992) found that the punching failure was more likely to occur at the interior than at the exterior connections, which generally experience a flexural-torsional type of failure. By reviewing the experimental data of 40 interior and 41 exterior connections, Luo and Durrani (1993) found that the eccentric shear stress model developed by Di Stasio and Van Buren (1960) predicted the punching capacity of the interior with reasonable accuracy. The ratio $v_{max}/(4\sqrt{f_c'})$ was found to have a mean of 1.00 and a standard deviation of 0.12. For square columns, the limit-state function for punching failure at interior connections can be expressed as

$$G_i(\mathbf{X}) = B(0.625f_{sp}) - \left\{\frac{V_u}{A_c} + 0.4[M_{un}(c_1 + d_{ave})/2J]\right\} \quad (12)$$

in which B = model uncertainty factor (measured shear strength/nominal shear strength); V_u = ultimate shear force; and M_{un} = unbalanced moment produced by combined earthquake and gravity loads or by gravity loads only. Analysis of the experimental results of footings and slab-column connections subjected to pure gravity shear [reported by the ACI-ASCE committee 326 ("Shear" 1962)] showed that the model uncertainty factor, $B = v_{max}/(4\sqrt{f_c'})$ (psi units), had a mean of 1.65 and a standard deviation of 0.27. The probability distributions of the model uncertainty factors, B, for pure gravity load and combined gravity and lateral loads are shown in Fig. 3.

The punching failure of the three- and 10-story flat-slab buildings is defined as the punching failure at one or more interior connections, i.e., the failure event of the building corresponds with the union of the punching failure of the individual interior connections. Therefore, the series system G-function is

$$G_s(\mathbf{X}) = \min[G_1(\mathbf{X}), G_2(\mathbf{X}), \ldots, G_m(\mathbf{X})] \quad (13)$$

ANALYSIS RESULTS

Gravity Loads Only

In the older ACI 318 building codes (ACI 318-41 to 318-63), the allowable shear stress at the slab critical section, defined at a distance of slab thickness minus 1.5 in. from the column face, was specified based on test results on the punching strength of slab-column connections subjected to gravity loads only. Because the punching capacity and failure mechanisms of slab-column connections subjected to combined gravity shear and unbalanced moment was not clearly understood at that time, the allowable shear stress of slab at connections was subjectively made overly conservative to compensate for the effects of unbalanced moment neglected in the shear stress calculations.

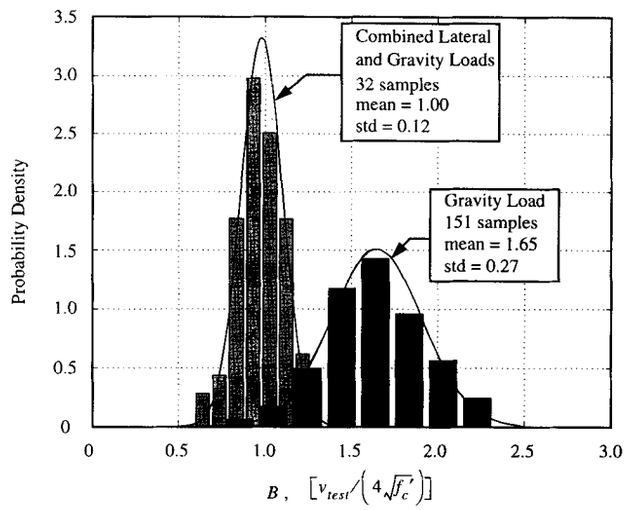

FIG. 3. Model Uncertainty Factor for Punching Failure at Interior Connections

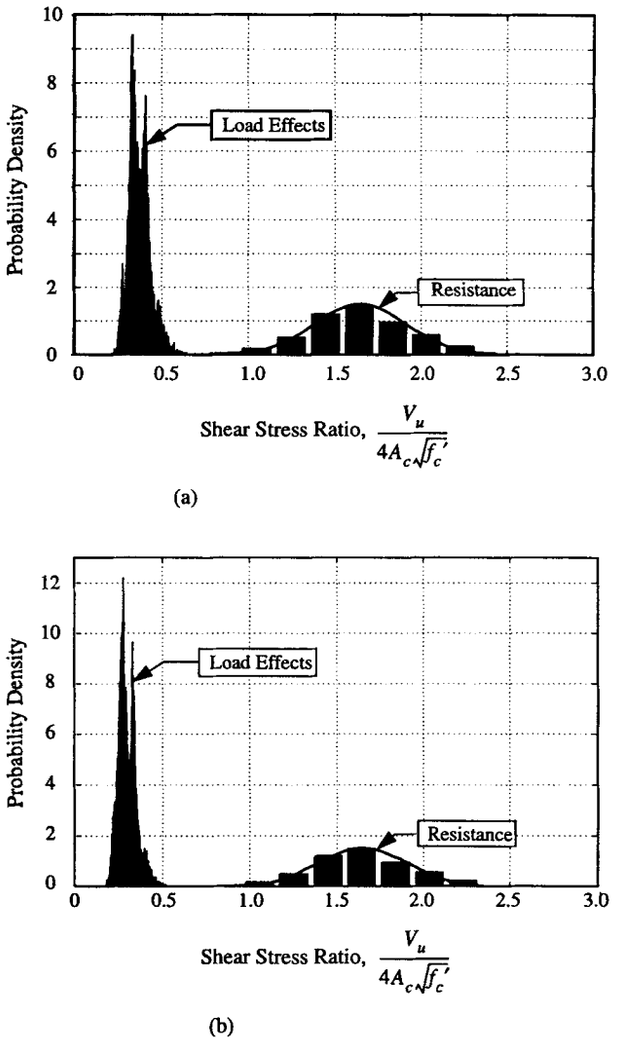

FIG. 4. Probability Density of Shear Stress Ratio for Interior Connections under Static Loads: (a) 50-yr Maximum Live Load; (b) Sustained Live Load

For the three- and 10-story flat-slab buildings subjected to uniformly distributed gravity loads only, the probability of punching failure and the corresponding reliability index β for both buildings are 2.97×10^{-6} and 4.528, respectively, for the 50-yr maximum live load. As shown in Figs. 4(a) and 4(b), the maximum shear stress ratio, $v_{max}/(4\sqrt{f_c'})$ (psi units) at the interior connections of the top three stories, has a mean and standard deviation of 0.371 and 0.061, respectively. For the combination of dead load plus sustained live load, the probability of punching and the reliability index β are 5.05×10^{-7} and 4.890, respectively. These results suggest that the flat-slab buildings under pure gravity loads have a relatively high reliability index β against punching failure, compared with the commonly accepted range of $\beta = 3.0 \sim 4.0$. Because the buildings are invariably subjected to lateral loads such as wind load and/or seismic load, the actual reliability index is expected to be smaller than the foregoing values.

The effect of the mean and standard deviation of the basic variables on the probability of punching failure and the β index are expressed by the sensitivity factors. The parametric sensitivity results for the reliability index β and the failure

TABLE 2. Sensitivity of Reliability Index β and Failure Probability P_f

X_i (1)	β		P_f	
	$\frac{\partial \beta}{\partial \mu_{x_i}} \sigma_{x_i}$ (2)	$\frac{\partial \beta}{\partial \sigma_{x_i}} \sigma_{x_i}$ (3)	$\frac{\partial P_f}{\partial \mu_{x_i}} \sigma_{x_i}$ (4)	$\frac{\partial P_f}{\partial \sigma_{x_i}} \sigma_{x_i}$ (5)
h_s	0.078 ~ 0.080	0.078 ~ 0.080	−0.078 ~ −0.080	−0.030 ~ −0.029
d_{ave}	−0.214 ~ −0.273	−0.214 ~ −0.273	0.214 ~ 0.273	−0.224 ~ −0.337
f_c'	—	—	—	—
f_{sp}	−0.227 ~ −0.293	−0.227 ~ −0.293	0.227 ~ 0.293	−0.250 ~ −0.388
A_s	—	—	—	—
f_s	—	—	—	—
c_1	−0.008 ~ −0.010	−0.008 ~ −0.010	0.008 ~ 0.010	0.000 ~ 0.000
c_2	−0.008 ~ −0.010	−0.008 ~ −0.010	0.008 ~ 0.010	0.000 ~ 0.000
L_s	0.090	0.090	−0.094	0.001
L_{50yr}	0.085	−0.085	−0.083	−0.017
B	−0.943 ~ −0.909	−0.943 ~ −0.909	0.943 ~ 0.909	−4.327 ~ −3.735

TABLE 3. Results for Interior Connections of Three-Story Building [Sues et al.'s (1985) Parameters]

Live load (1)	a_p[a] (g) (2)	Soil type (3)	Punching Failure P_f (4)	Punching Failure β (5)	$v_{max}/(4\sqrt{f_c'})$ Mean (6)	$v_{max}/(4\sqrt{f_c'})$ Standard deviation (7)	Drift Ratio (%) Mean (8)	Drift Ratio (%) Standard deviation (9)
L_{50yr}	0.00	—	2.97×10^{-6}	4.528	0.371	0.061	—	—
L_{sus}	0.00	—	5.05×10^{-7}	4.890	0.297	0.051	—	—
L_{sus}	0.05	Hard	3.67×10^{-3}	2.681	0.566	0.098	0.131[b]/0.176[c]	0.034/0.044
		Intermediate	5.09×10^{-3}	2.570	0.580	0.098	0.141[b]/0.187[c]	0.035/0.045
		Soft	9.03×10^{-3}	2.364	0.608	0.098	0.157[b]/0.200[c]	0.035/0.045
	0.10	Hard	4.10×10^{-2}	1.739	0.695	0.107	0.252[b]/0.331[c]	0.062/0.080
		Intermediate	4.51×10^{-2}	1.695	0.709	0.107	0.267[b]/0.347[c]	0.062/0.082
		Soft	7.50×10^{-2}	1.439	0.739	0.114	0.301[b]/0.379[c]	0.068/0.091
	0.15	Hard	9.93×10^{-2}	1.286	0.780	0.121	0.385[b]/0.509[c]	0.107/0.150
		Intermediate	1.17×10^{-1}	1.188	0.792	0.123	0.412[b]/0.546[c]	0.115/0.165
		Soft	1.56×10^{-1}	1.012	0.825	0.132	0.493[b]/0.646[c]	0.140/0.209
	0.20	Hard	1.81×10^{-1}	0.911	0.838	0.140	0.559[b]/0.754[c]	0.186/0.273
		Intermediate	1.93×10^{-1}	0.865	0.850	0.141	0.596[b]/0.809[c]	0.195/0.288
		Soft	2.71×10^{-1}	0.610	0.888	0.156	0.742[b]/0.999[c]	0.239/0.360

[a]Expected peak ground acceleration.
[b]Roof drift ratio = displacement at roof/total height.
[c]Maximum story drift ratio = maximum interstory drift/story height.

TABLE 4. Results for Interior Connections of Three-Story Building [Lai's (1982) Parameters]

Live load (1)	a_p[a] (g) (2)	Soil type (3)	Punching Failure P_f (4)	Punching Failure β (5)	$v_{max}/(4\sqrt{f_c'})$ Mean (6)	$v_{max}/(4\sqrt{f_c'})$ Standard deviation (7)	Drift Ratio (%) Mean (8)	Drift Ratio (%) Standard deviation (9)
L_{sus}	0.05	Rock	2.80×10^{-3}	2.770	0.534	0.092	0.093[b]/0.132[c]	0.025[b]/0.035[c]
		Soil	4.95×10^{-3}	2.579	0.575	0.094	0.130[b]/0.168[c]	0.030[b]/0.039[c]
	0.10	Rock	1.79×10^{-2}	2.099	0.646	0.101	0.191[b]/0.271[c]	0.048[b]/0.063[c]
		Soil	3.38×10^{-2}	1.827	0.697	0.102	0.251[b]/0.327[c]	0.052[b]/0.070[c]
	0.15	Rock	5.48×10^{-2}	1.600	0.724	0.111	0.278[b]/0.390[c]	0.072[b]/0.097[c]
		Soil	1.01×10^{-1}	1.274	0.777	0.116	0.371[b]/0.494[c]	0.089[b]/0.130[c]
	0.20	Rock	1.08×10^{-1}	1.235	0.781	0.121	0.380[b]/0.535[c]	0.113[b]/0.160[c]
		Soil	1.57×10^{-1}	1.009	0.831	0.130	0.521[b]/0.721[c]	0.153[b]/0.236[c]

[a]Expected peak ground acceleration.
[b]Roof drift ratio.
[c]Maximum story drift.

probability P_f are provided as by-products of the reliability analysis and are given in Table 2. The variables influencing the reliability index the most are the model uncertainty factor, the concrete splitting strength, and the slab effective depth.

Seismic Loading

Tests on slab-column connections have shown that the unbalanced moment at the connection is transferred through a combination of flexural and shear mechanisms. The portion of the unbalanced moment transferred through shear is assumed to result in a linearly varying shear stress at the critical section. When the maximum shear stress due to gravity and lateral loads reaches $(4\sqrt{f_c'})$ (psi units) at the critical section, the connection is believed to have reached its punching shear capacity. To determine the reliability against punching failure, the unbalanced moment produced by earthquakes needs

TABLE 5. Results for Interior Connections of 10-Story Building

Live load (1)	a_p[a] (g) (2)	Soil type (3)	Punching Failure P_f (4)	Punching Failure β (5)	$v_{max}/(4\sqrt{f'_c})$ Mean (6)	$v_{max}/(4\sqrt{f'_c})$ Standard deviation (7)	Drift Ratio (%) Mean (8)	Drift Ratio (%) Standard deviation (9)
L_{sus}	0.05	Soil [Lai (1982)]	1.13×10^{-2}	2.279	0.638	0.093	0.119[b]/0.212[c]	0.032[b]/0.056[c]
		Intermediate [Sues et al. (1985)]	1.33×10^{-2}	2.216	0.642	0.096	0.141[b]/0.230[c]	0.058[b]/0.082[c]
	0.10	Soil [Lai (1982)]	7.88×10^{-2}	1.413	0.769	0.103	0.253[b]/0.449[c]	0.09[b]/0.145[c]
		Intermediate [Sues et al. (1985)]	1.14×10^{-1}	1.206	0.795	0.120	0.309[b]/0.480[c]	0.121[b]/0.193[c]
	0.15	Soil [Lai (1982)]	2.12×10^{-1}	0.802	0.858	0.136	0.449[b]/0.785[c]	0.177[b]/0.369[c]
		Intermediate [Sues et al. (1985)]	2.34×10^{-1}	0.726	0.884	0.158	0.552[b]/0.897[c]	0.210[b]/0.412[c]
	0.20	Soil [Lai (1982)]	3.23×10^{-1}	0.459	0.912	0.158	0.641[b]/1.111[c]	0.226[b]/0.509[c]
		Intermediate [Sues et al. (1985)]	4.01×10^{-1}	0.250	0.953	0.184	0.867[b]/1.486[c]	0.250[b]/0.551[c]

[a]Expected peak ground acceleration.
[b]Roof drift ratio.
[c]Maximum interstory drift ratio.

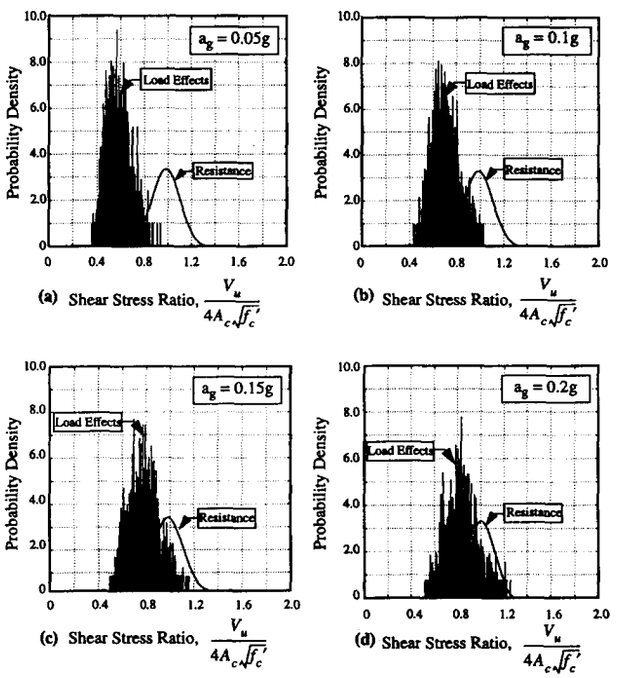

FIG. 5. Probability Density of Shear Stress Ratio for Three-Story Building under Combined Gravity and Seismic Loads [Lai's (1982) Soil Parameters]

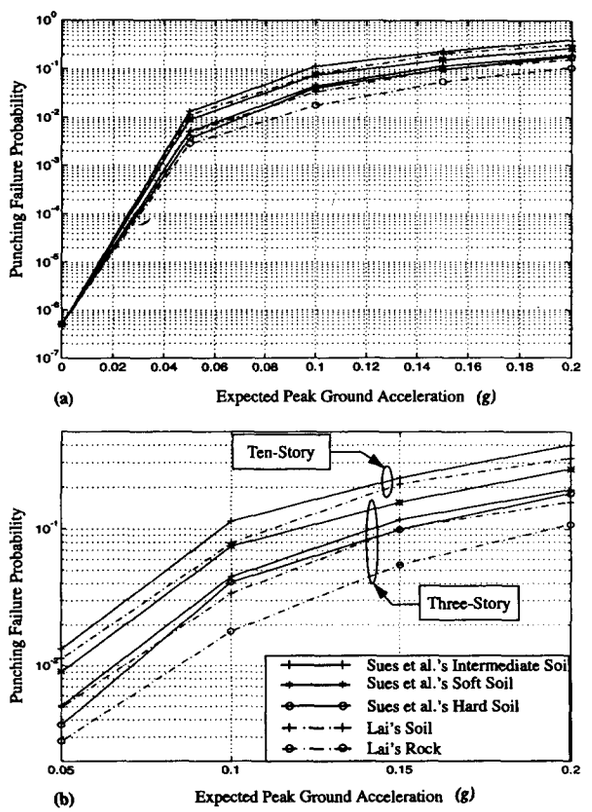

FIG. 6. Probability of Punching Failure at Interior Connections

to be calculated first. In this study, the unbalanced moment was obtained by performing a two-dimensional (2D) nonlinear response analysis of the three- and 10-story flat-slab buildings under earthquake excitations. The computer program for the inelastic damage analysis of reinforced-concrete frame-shear-wall structures, IDARC-version 3 (Kunnath et al. 1992), was used for the nonlinear analysis. The flat-slab buildings are modeled as equivalent frames in which the floor slabs are replaced by equivalent beams (Luo and Durrani 1995). In the IDARC program, the rules for inelastic loading reversals are described by combining a trilinear envelope with four parameters: stiffness degrading coefficient, energy-based deteriorating coefficient, ductility-based deteriorating coefficient, and target slip or crack-closing parameter (Kunnath et al. 1992). These hysteretic parameters were identified from the measured hysteretic response of four nonductile slab-column subassemblies tested by Durrani and Du (1992). The validity of this approach was verified by comparing the simulated load-drift response with the measured response of the tested nonductile slab-column subassemblies (Luo et al. 1994).

The probability of punching failure at the interior connections of the flat-slab buildings may be evaluated in terms of the conditional probability. For a given expected peak ground acceleration, Monte Carlo simulations were performed for each building to evaluate the failure probability against punching. Expected peak ground accelerations ranging from $0.05g$ to $0.2g$ were selected to represent the earthquakes of the eastern United States where most of the older flat-slab buildings are situated. By considering the variability in slab and column dimensions, strengths of concrete and steel and by taking into account the model uncertainty, the live-load

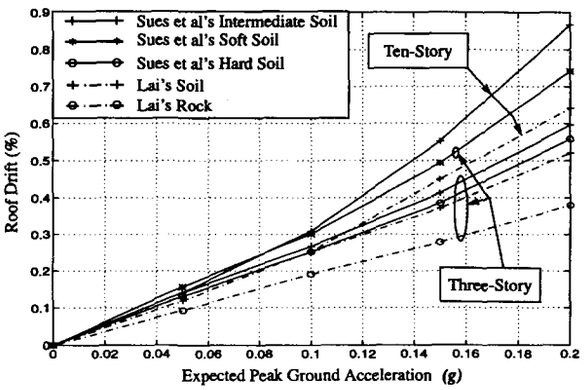

FIG. 7. Expected Drift Levels for Different Ground Accelerations: (a) Roof Drift versus Ground Acceleration; (b) Maximum Story Drift versus Ground Acceleration

dispersion, and the randomness of the earthquake ground acceleration time history, the failure probability and reliability index were estimated based on the simulated population of the shear stress ratios, $v_{max}/(4\sqrt{f'_c})$ (psi units). The results are summarized in Tables 3–5 in terms of the expected peak ground accelerations and the soil conditions. A representative sample of probability-density distributions of the shear stress ratio at interior connections for the three-story flat-slab building is shown in Fig. 5. The reliability index β for punching failure at the interior connections of both the three- and 10-story frames varies from 2.77 to 0.61 for an expected peak ground acceleration varying from $0.05g$ to $0.2g$. The effect of infills and claddings were not considered in these analyses. The combination of soft soil and the highest expected peak ground acceleration gave the lowest reliability index for the flat-slab buildings of both heights. The probability of punching failure for the three- and 10-story buildings with respect to expected peak ground accelerations and soil types is shown in Fig. 6. The 10-story flat-slab building has a relatively higher probability of punching failure at interior connections compared with the three-story building. As expected, the probability of failure increases with an increasing expected peak ground acceleration.

The interstory drift is an important parameter in evaluating the response of existing flat-slab buildings. The interstory drift ratios for the three- and 10-story flat-slab buildings vary from 0.13% to 1.5% depending on the soil condition and the magnitude of ground acceleration, as shown in Fig. 7. For an expected peak ground acceleration of $0.15g$, the maximum interstory drift ratio of the 10-story flat-slab building was 0.9% for the intermediate soil, which is significantly higher than the allowable drift of 0.5% specified by *UBC* (1991). The maximum interstory drift ratio for the two buildings was less than 0.5% for expected peak ground accelerations smaller than $0.1g$ and larger than 0.5% for expected peak ground accelerations larger than $0.2g$.

The influence of the local soil parameters ω_g and ξ_g on the failure probability and the drift was also studied. The ground parameters suggested by Sues et al. (1985) yielded higher drift ratios and lower reliability indices compared with the parameters suggested by Lai (1982).

CONCLUSIONS

The reliability of flat-slab buildings designed only for gravity loads was investigated for punching failure at interior slab-column connections under pure gravity load and under combined gravity and seismic loads. The reliability index for typical three- and 10-story flat-slab buildings designed according to ACI 318-56 was calculated by FORM/SORM analysis and by the Monte Carlo simulation. The artificial earthquake ground acceleration time histories were generated from the Kanai-Tajimi power spectral density. The member dimensions, material strengths, and live load were treated as random variables. Model uncertainty was included in the limit-state function. The following conclusions are drawn based on the results of this investigation.

The reliability indices of the older flat-slab buildings against punching failure at interior connections under the 50-yr maximum live load and sustained live load were found to be 4.53 and 4.89, with corresponding failure probabilities of 2.97×10^{-6} and 5.05×10^{-7}, respectively. The low probability of failure affirms the safety of these buildings under pure gravity loads.

A sensitivity study with respect to the basic variables indicated that the reliability indices for punching failure under the gravity load only were most sensitive to the model uncertainty, the splitting strength of concrete, and the effective slab depth.

Under seismic loading, the probability of punching failure increased with increasing expected peak ground acceleration and the number of stories in the building. For a peak ground acceleration of $0.05g$, the probability of punching failure for the three- and 10-story flat-slab buildings was 5×10^{-3} and 1.0×10^{-2}, respectively, for intermediate soil. However, when the expected peak ground acceleration is raised to $0.2g$, these probabilities of failure increased significantly to 0.18 and 0.32, respectively.

The local soil conditions have a significant effect on the probability of punching failure. The study indicated that the probability of failure of flat-slab buildings on soft soil was about 1.5 times the probability of failure on hard soil.

The choice of the Kanai-Tajimi frequency and damping parameters affected the calculated values of reliability indices. As such, the reliability indices must be compared in conjunction with the Kanai-Tajimi parameters used in the analysis.

APPENDIX I. REFERENCES

Ang, A. H.-S., and Cornell, C. A. (1974). "Reliability bases of structure safety and design." *J. Struct. Engrg.*, ASCE, 100(9), 1755–1769.

Building code requirements for reinforced concrete. (1956). *ACI 318-56*, American Concrete Institute (ACI), Detroit, Mich.

Building code requirements for reinforced concrete. (1989). *ACI 318-89*, American Concrete Institute (ACI), Detroit, Mich.

Chalk, P. L., and Corotis, R. B. (1976). "Probability model for design live loads." *J. Struct. Engrg.*, ASCE, 106(10), 2017–2032.

Corotis, R. B., and Doshi, V. A. (1977). "Probability models for live-load survey results." *J. Struct. Engrg.*, ASCE, 103(6), 1257–1273.

"CSMIP strong-motion records from the Whittier, California earthquake of 1 October, 1987." (1987). *Rep. OSMS 87-05*, Calif. Dept. of Conservation, Div. of Mines and Geology, Sacramento, Calif.

Culver, C. G. (1976). "Live-load survey results for office buildings." *J. Struct. Engrg.*, ASCE, 102(12), 2269–2284.
Di Stasio, J., and Van Buren, M. P. (1960). "Transfer of bending moment between flat slab floor and column." *ACI J.*, 57(3), 299–314.
Durrani, A. J., and Du, Y. (1992). "Seismic resistance of slab-column connections in existing non-ductile flat-slab buildings." *Tech Rep. NCEER-92-0010*, State Univ. of New York at Buffalo, N.Y.
Ellingwood, B. R., and Ang, A. H.-S. (1974). "Risk-based evaluation of design criteria." *J. Struct. Engrg.*, ASCE, 100(9), 1771–1788.
Ellingwood, B. R., and Culver, C. (1977). "Analysis of live loads in office buildings." *J. Struct. Engrg.*, ASCE, 103(8), 1551–1560.
Fiorato, A. E. (1973). "Geometric imperfections in concrete structures." *Nat. Swedish Build. Res. Document No. 5*, Chalmers Univ. of Technol., Gothenberg, Sweden.
Hwang, H. H. M., and Jaw, J. W. (1990). "Probabilistic damage analysis of structures." *J. Struct. Engrg.*, ASCE, 116(7), 1992–2007.
"Impressions of the Guerrero-Michoacan Mexico earthquake 19, September, 1985." *Preliminary Reconnaissance Rep.*, Earthquake Engrg. Res. Inst. (EERI), Oakland, Calif.
Julian, O. G. (1955). "Discussion of 'Strength variations in ready-mixed concrete,' by A. E. Cummings." *ACI J.*, 51(12), 772–778.
Kunnath, S. K., Reinhorn, A. M., and Lobo, R. F. (1992). "IDARC-version 3.0, a program for inelastic damage analysis of reinforced concrete structures." *Tech. Rep. NCEER-92-0022*, State Univ. of New York at Buffalo, N.Y.
Lai, S.-S. P. (1982). "Statistical characterization of strong ground motions using power spectral density function." *Bull. Seismological Soc. of Am.*, 72(1), 259–274.
Liu, P. L., Lin, H. Z., and Kiureghian, A. D. (1989). "CALREL: calculation of reliability." *Manual*, Dept. of Civ. Engrg., Univ. of Calif. at Berkeley, Calif.
Lu, R., Luo, Y. H., and Conte, J. P. (1994). "Evaluation of the reliability of R/C beam under bending, shear and torsion loading." *Struct. Safety*, Vol. 14, 277–298.
Luo, Y. H., and Durrani, A. J. (1994). "Seismic retrofit strategy for non-ductile flat-plate connections. *Proc., 5th U.S. Nat. Conf. on Earthquake Engrg.*, Earthquake Engrg. Res. Inst. (EERI), Oakland, Calif.
Luo, Y. H., Durrani, A. J., and Conte, J. P. (1994). "Equivalent frame analysis of flat plate buildings for seismic loading." *J. Struct. Engrg.*, ASCE, 120(7), 2137–2155.
Luo, Y. H., and Durrani, A. J. (1995a). "Equivalent beam model for flat-slab buildings. Part I: Interior connections." *ACI Struct. J.*, 92(1), 115–124.
Luo, Y. H., and Durrani, A. J. (1995b). "Equivalent beam model for flat-slab buildings. Part II. Exterior connections." *ACI Struct. J.*, 92(2), 250–257.
Mirza, S. A., Hatzinikolas, M., and MacGregor, J. G. (1979). "Statistical descriptions of strength of concrete." *J. Struct. Engrg.*, ASCE, 105(6), 1021–1036.
Mirza, S. A., and MacGregor, J. G. (1979a). "Variations in dimensions of reinforced concrete members." *J. Struct. Engrg.*, ASCE, 105(4), 751–765.
Mirza, S. A., and MacGregor, J. G. (1979b). "Variability of mechanical properties of reinforced bars." *J. Struct. Engrg.*, ASCE, 105(5), 921–937.
Moayyad, P., and Mohraz, B. (1982). "A study of power spectral density of earthquake accelerograms." *Res. Rep.*, Civ. and Mech. Engrg. Dept., Southern Methodist Univ., Dallas, Tex.
"Shear and diagonal tension: slabs and footings." (1962). *ACI J.*, 59(3), 353–396.
Shinozuka, M. (1974). "Digital simulation of random process in engineering mechanics with the aid of FFT technique." *Stochastic problems in mechanics*, S. T. Ariaratnam and H. E. E. Liepholz, eds., Univ. of Waterloo Press, Waterloo, Ontario, Canada.
Sues, R. H., Wen, Y. K., and Ang, A. H.-S. (1985). "Stochastic evaluation of seismic structural performance." *J. Struct. Engrg.*, ASCE, 111(6), 1204–1218.
Uniform building code. (1991). International Conference of Building Officials, Whittier, Calif.
Vanmarcke, E. H., and Lai, P. S.-S. (1980). "Strong-motion duration and RMS amplitude of earthquake records." *Bull. Seismological Soc. of Am.*, 70(4), 1293–1307.

APPENDIX II. NOTATION

The following symbols are used in this paper:

A_c = area of the slab critical section specified by ACI 318-89 (*Building* 1989);
B = model uncertainty factor;
c_1 = column dimension in the bending direction;
c_2 = column dimension normal to the bending direction;
d_{ave} = effective depth of slab;
f'_c = compressive strength of concrete;
f_{sp} = splitting strength of concrete;
f_y = yielding strength of steel;
h = slab thickness;
J = polar moment inertia of the slab critical section;
K_s = flexural stiffness of slab;
K_t = torsional stiffness;
L_s = sustained live load;
L_{50yr} = maximum live load with 50-yr return period;
l_1 = span length in the bending direction, center to center of columns;
l_2 = span length in the direction transverse to l_1, center to center of columns;
M_{um} = unbalanced moment at an interior slab-column connection;
V_u = shear force due to gravity and lateral loads;
v_{max} = maximum shear stress at critical section;
α = stiffness degrading coefficient;
α_i = effective slab-width factor for slab at interior connection;
α_e = effective slab-width factor for slab at exterior connection;
β = reliability index;
ξ_g = critical sampling of site soil;
ω_g = dominant ground frequency of site soil and;
χ = stiffness reduction factor for gravity load.